Trieu Khoa Nguyen [ID] [1], Minh Quang Chau [ID] [1], The-Can Do,[2]
Anh-Duc Pham [ID] [2]

Characterization of geometrical parameters of plastic bottle shredder blade utilizing a two-step optimization method

In this paper, a numerical and experimental investigation of geometrical parameters of the blade for plastic bottle shredder was performed based on the Taguchi method in combination with a response surface method (RSM). Nowadays, plastic waste has become a major threat to the environment. Shredding, in which plastic waste is shredded into small bits, ready for transportation and further processing, is a crucial step in plastic recycling. Although many studies on plastic shredders were performed, there was still a need for more researches on the optimization of shredder blades. Hence, a numerical analysis was carried out to study the influences of the relevant geometrical parameters. Next, a two-step optimization process combining the Taguchi method and the RSM was utilized to define optimal parameters. The simulation results clearly confirmed that the current technique can triumph over the limitation of the Taguchi method, originated from a discrete optimization nature. The optimal blade was then fabricated and experimented, showing lower wear via measurement by an ICamScope® microscope. Hence, it can be clearly inferred from this investigation that the current optimization method is a simple, sufficient tool to be applied in such a traditional process without using any complicated algorithms or expensive software.

1. Introduction

Nowadays, plastic has become one of the most commonly used materials in the world [1]. Therefore, plastic waste has become a major threat to the environment due to its long decay time, a huge amount of waste generated, non-biodegradability

✉ Trieu Khoa Nguyen, e-mails: nguyenkhoatrieu@iuh.edu.vn, ducpham@dut.udn.vn

[1]Faculty of Mechanical Engineering, Industrial University of Ho Chi Minh City, Ho Chi Minh City, Vietnam. ORCIDs: T.K.N.: 0000-0003-2922-1512; M.Q.C: 0000-0002-3180-3311

[2]Faculty of Mechanical Engineering, The University of Danang – University of Science and Technology, Da Nang City, Vietnam. ORCID A-D.P.: 0000-0002-0400-9200

and the depletion of natural resources [2]. Hence, the need for plastic recycling, whereby some of the recyclable plastics are processed for re-use, is increasing day by day. Recycling is one of the most promising actions necessary to reduce the environmental impact of plastic waste, as it reduces carbon dioxide emission, oil usage and quantity of waste to be disposed [3]. In waste plastic recycling, to enhance its portability, easiness and readiness to be utilized in other new products, the waste must be reduced to smaller particle sizes using a shredder.

Because of the importance of the shredding process, there have been many investigations regarding design and development of plastic shredders. Ayo, A., Olukunle, O. J., & Adelabu, D. J. from Nigeria [2] developed a low-cost waste plastic shredding machine for small and medium scale manufactories working on recycled plastics. The machine was also evaluated at three working speeds for average particle sizes. Reddy, S., & Raju, T. [4] also built a mini plastic shredder machine. They claimed that the machine was simple, efficiency and low cost. However, the blades and the working conditions of the machine were not analyzed yet. The works in [5–11] had the same situation that the machines were not evaluated for performance yet. While Jassim M. Abdulkarim Jaff et al. [12] designed and fabricated both shredder/crusher and extruder for their plastic recycling system. Farayibi, P. K. et al. [3] also presented a conceptual design for a plastic recycling machine. The structural analysis was then performed using a finite element analysis (FEA) tool in SolidWorks Computer Aided Design (CAD) application. However, the obtained maximum stress did not contributed much to the development and evaluation of the machine.

In a shredder, the cutting blade plays a vital role in the shredding process because it determines the size of shredded pieces. Furthermore, it is a crucial factor that affects the working efficiency and life-time of the machine [13]. However, geometrical parameters of the cutting blade and their effects on the wear and/or displacement have not been investigated enough. In [13], S. Yadav et al. carried out displacement analysis and equivalent stress analysis. Nevertheless, these results were not used for any further evaluation or optimization. In the same manner, Sekar Ravi [14] performed total displacement, stress and strain analysis using the static structural method. After that, the cutting blade was improved by a hardening method or chrome plating or improving the properties of the blades. Nasr, M. F., & Yehia, K. A. [15] and Yepes, C. P. et al. [16] also analyzed static stress within a given shredder blade with three and two cutting edges, respectively, used for shredding PET (polyethylene terephthalate) waste plastic. And in [17], A. Ikpe et al. simply examined the variations of stress distribution at different force values using SolidWorks® without any further utilization of this obtained information.

Because this inadequacy, a newly two-step optimization technique that integrates both the Taguchi method [18] and the RSM [19] was applied in this study. The Taguchi method and RSM are commonly used methods to obtain the optimized values of the related parameters [20]. However, utilizing a single one of these two

methods does not yield precise optimization due to the discrete property of the Taguchi method [21, 22] and the complicated nature of the geometry of the blade.

The Taguchi method was firstly applied with concern for the important geometrical parameters of the shredding blade, giving out intermediate optimum results. These achieved results were then employed for a subsequent RSM step to define the finely tuned optimum values. With this combination method, the influences of geometrical parameters on wear / displacement of the shredding blade were studied utilizing the conditions that resulted in minimal wear / displacement.

2. Description of the shredding blade

In this investigation, the displacement / wear phenomenon of the shredding blade of the plastic waste shredder, as illustrated in Fig. 1, was investigated. The shredder, which is single-shaft type, included 14 cutting blades, as shown in Fig. 2. Fig. 2a shows the design of the shredding blade. It was designed to have an S-shape with two shredding ends and a hexagonal hole in the center for fixing the drive shaft. The letters in Fig. 2a show the symbols of factors used in this study. Fig. 2b shows a photograph of the blade produced by laser cutting and grinding process. It should be noted that, while our blade has the same S-shape as the announced blade, the tip of it has been improved. The tip of the blade is made by two curves, then diagonally cut, as shown in the detailed portion in Fig. 3, to increase the hardness of the tip. At the same time, this diagonal cut allows the blade to be sharpened without removing the blade, shortening maintenance and repair time. Furthermore, the sharpening process does not change the outer diameter of the blade, the dimension R60 in Fig. 2a. In other types of blades, plastic is likely to get caught in the gap between the blade and the wall of the shredder when the outer diameter of the blade is changed.
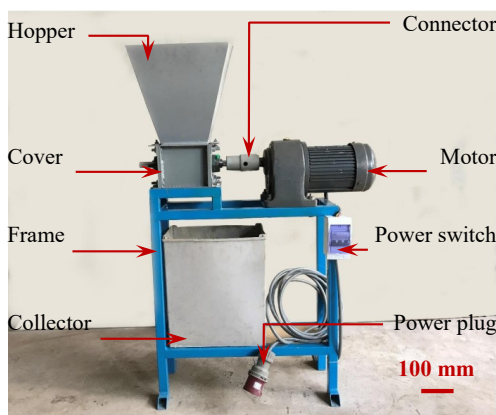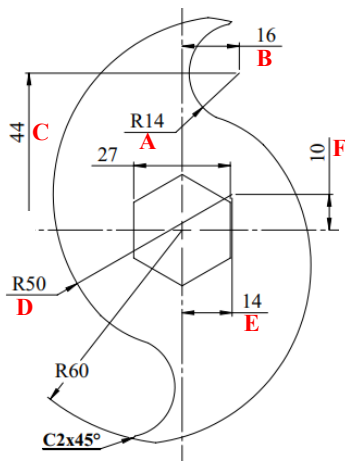

Fig. 1. Photograph of the plastic waste shredder developed in the current investigation

(a) illustration of the shredding blade   (b) photograph of a fabricated shredding blade

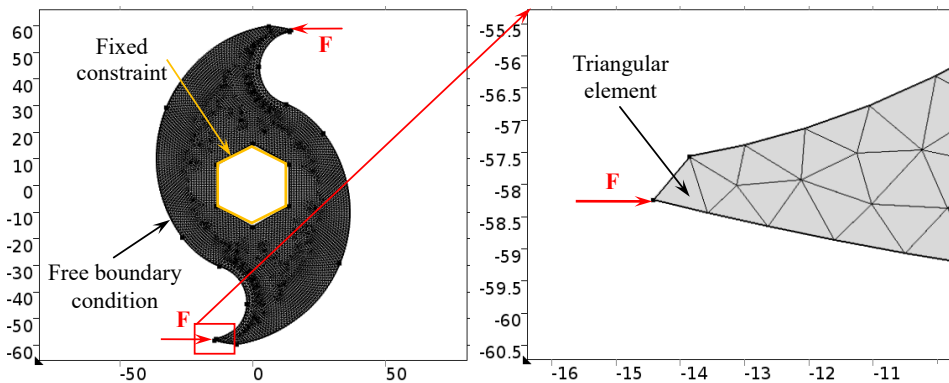Fig. 2. The designed shredding blade of the plastic waste shredder

Fig. 3. The meshed shredder blade and the boundary conditions

The material used for the shredding blades was S45C steel of 5 mm thickness. The material was selected for the cost reduction reason, to be suitable for small-size manufactories. Before finely final machining, the blades were heat-treated for better properties. The volumetric quenching (or body quenching) method was utilized for the blades in this study by a local company. Table 1 presents the important properties of the material used in the numerical analysis.

For the numerical study, a 2D geometrical model was built for the entire shredding blade. In this investigation, the triangular elements were utilized to discretize the simulation / computational domain, as shown in Fig. 3. The model was constructed with 9892 triangular elements, 376 edge elements and 20 vertex elements.

Properties of S45C steel after heat treatment utilized in the numerical analysis

	Value	Unit
Density	7.78×10^3	kg/m^3
Young's modulus	460	GPa
Poisson's ratio	0.3	–
Coefficient of thermal expansion	12.5	1/K

The plastic bottle used for this experiment was the most popular local disposable water drinking bottle, made of polyethylene terephthalate (PET) material. The maximum required cutting force was calculated from the tensile strength of the PET material (58.6–72.4 MPa [23]), the thickness, and the diameter of the plastic bottle. The result showed that the maximum force acting on the tip of the blade during the shredding process was 1809.54 N. It should be noted that the caps of the plastic bottles, which were usually made of polypropylene (PP), were removed prior to the experiments.

3. Numerical methods

3.1. Displacement simulation

In the current investigation, a multiphysics analysis software, Comsol®, was utilized to analyze the displacement of the blade. During the shredding process, the displacement of the shredding blades originated from the shredding resistance as the plastic bottles were shredded into small pieces. To accurately analyze the displacement phenomenon, the analysis tool utilizes a linear elastic solid model (isotropic type) with a linear elastic material. The equations are shown below:

$$-\nabla \cdot \sigma = F_v, \tag{1}$$

$$\sigma = s, \tag{2}$$

where σ or s is the stress, $\nabla\cdot$ is the divergence, F_v is force per unit volume.

The Duhamel-Hooke's law refers the stress tensor to the strain tensor and the temperature:

$$s - s_0 = C : (\varepsilon - \varepsilon_0 - \alpha\theta). \tag{3}$$

where s_0 and ε_0 are the initial stress and strain, C is the 4-th order elasticity tensor, ":" is the double-dot tensor product (or double contraction), α is the thermal expansion tensor, and $\theta = T - T_{\text{ref}}$.

The total strain tensor is described in terms of the displacement gradient:

$$\varepsilon = \frac{1}{2}\left[(\nabla u)^T + \nabla u\right], \tag{4}$$

∇ is the gradient and u denotes the displacement.

3.2. Optimization using Matlab

Optimization of the geometries can be considered as a calculation of the dimensions that maximizes or minimizes a target property while satisfying all constraints. In the case of this investigation, the optimization problem is utilized to define the relevant dimensions giving out minimal displacement of the shredding blade. A common non-linear constrained optimization problem requires determining a vector $\vec{x}$ that is a local minimum to a scalar function $f(\vec{x})$ subject to constraints within the acceptable values of $\vec{x}$; as [20]:

$$\text{find} \quad \min_{\vec{x}} f(\vec{x}) \quad \text{such that} \begin{cases} c(\vec{x}) \leqslant 0, \\ c_{\text{eq}}(\vec{x}) = 0, \\ A \cdot \vec{x} \leqslant b, \\ A_{\text{eq}} \cdot \vec{x} = b_{\text{eq}}, \\ l_b \leqslant \vec{x} \leqslant u_b, \end{cases} \tag{5}$$

where c contains the nonlinear inequalities evaluated at x, c_{eq} contains the nonlinear equalities evaluated at x; A and b are the matrix and vector for linear inequality constraints; while A_{eq} and b_{eq} are the matrix and the vector for linear equality constraints, respectively; l_b is the vector of lower bounds, and u_b is the vector of upper bounds.

In this investigation, a short MATLAB® script was developed to identify the optimum values of the considered geometrical parameters. The "fmincon" function and "for" loop were utilized in this study. Because the calculated values from "fmincon" function varied relying on the starting point of the optimization, the range of the parameters was split into several sub-ranges with a designated beginning point for each. With this method, a convergence into a local optimum could be evaded, and a global optimum within the range was instead achieved.

4. Results and discussion

4.1. Effect of dimensions

4.1.1. Selection of dimensions

There are many dimensions which form the shape of the blade. However, only the dimensions which form the shredding ends were taken into account and considered in the initial approach towards optimization. It is worth noting that the outer diameter of the blade, 120 mm, was maintained during the optimization process. As a continuation of previous works, the current investigation re-used the shredder, except for the blades. Moreover, three levels of each factor were set based on the preliminary test. Table 2 lists the dimensions and the three levels of them used in this investigation. Because the dimensions were mutually constrained, the levels

Processing parameters and their detailed conditions investigated in the present study

Symbol	Factor	Level		
		1	2	3
A	Diameter $\varnothing 28$ (mm)	27.8	28	28.2
B	The x coordinate of $\varnothing 28$ (mm)	15.8	16	16.2
C	The y coordinate of $\varnothing 28$ (mm)	43.8	44	44.2
D	Diameter $\varnothing 100$ (mm)	99.8	100	100.2
E	The x coordinate of $\varnothing 100$ (mm)	13.8	14	14.2
F	The y coordinate of $\varnothing 100$ (mm)	9.8	10	10.2

in Table (2) were chosen so that the blade remained S-shaped. Using this method, a DOE-based study and response surface model could be systematically built.

From the quantity of chosen dimensions and their respective levels, a subset of the $L_{18}(3^6)$ orthogonal array was chosen, as described in Table 3 After that, 18 numerical simulations for the blades under the impact of the shredding force

Orthogonal array utilized in the current investigation: Detailed conditions and maximum displacement achieved by the numerical simulation (MSD is mean standard deviation)

No.	Factors						Displacement (µm)	MSD	S/N ratio
	A	B	C	D	E	F			
1	1	1	1	1	1	1	0.18830	0.035458	14.50286
2	1	2	2	2	2	2	0.17801	0.031689	14.99093
3	1	3	3	3	3	3	**0.16526**	0.027312	15.63641
4	2	1	1	2	2	3	0.17734	0.031449	15.02393
5	2	2	2	3	3	1	0.18509	0.03426	14.65219
6	2	3	3	1	1	2	0.17414	0.030326	15.18182
7	3	1	2	1	3	2	0.19171	0.036752	14.34714
8	3	2	3	2	1	3	0.17207	0.029608	15.2859
9	3	3	1	3	2	1	0.17917	0.032102	14.93467
10	1	1	3	3	2	2	0.18201	0.033129	14.79794
11	1	2	1	1	3	3	0.17490	0.030592	15.14398
12	1	3	2	2	1	1	0.17024	0.028982	15.37867
13	2	1	2	3	1	3	0.17542	0.030771	15.1186
14	2	2	3	1	2	1	0.19575	0.038318	14.16597
15	2	3	1	2	3	2	0.17729	0.031432	15.02627
16	3	1	3	2	3	1	0.20187	0.040751	13.89862
17	3	2	1	3	1	2	0.17725	0.031417	15.02832
18	3	3	2	1	2	3	0.17597	0.030964	15.09141
Sum							3.24181	0.585313	
Average							0.18010		14.90031

were performed utilizing the dimension combinations of the orthogonal array. The boundary conditions for these simulations were shown in Fig. 3, in which "free boundary condition" meant that it was let to be deformed freely. The maximum displacements of the blades, calculated by the numerical simulations, and the corresponding S/N ratios were also described in Table 3. Because the displacement, the objective characteristic of the investigation, should be minimized to obtain an effective shredding process, the "smaller-the-better" description of the S/N ratio was utilized for determining each S/N ratio.

4.1.2. Contribution of geometrical factors

Table 4 presents the outlined S/N ratio outcomes for each factor. The outcomes are also shown in Fig. 4, which clearly illustrates the influences of the factors. For instance, the displacement of the shredding end of the blade was found to increase with increasing diameter $\varnothing 28$ (factor A), the x coordinate of $\varnothing 100$ (factor E) and decreasing the x coordinate of $\varnothing 28$ (factor B), the y coordinate of $\varnothing 100$ (factor F) within the typical regime of utilization. The reason was that when these factors change as above, the tip region of the blade became smaller and thinner. As a result, the stress in the tip of the blade increased. Hence, the displacement was increased accordingly. By considering the difference between the minimum and maximum

Table 4.

S/N ratio results of each factor

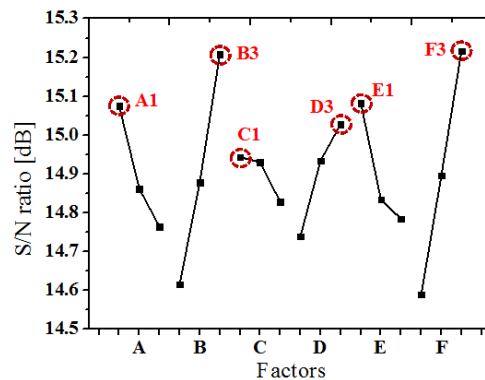| Factors	A	B	C	D	E	F	Total
Level 1	15.07513	14.61485	14.94334	14.73886	15.08269	14.58883	
Level 2	14.86146	14.87788	14.92982	14.93405	14.83414	14.89540	44.70093
Level 3	14.76434	15.20821	14.82778	15.02802	14.78410	15.21671	
Difference	0.31079	0.59336	0.11556	0.28916	0.29859	0.62788	2.23534
Contribution %	13.90	26.54	5.17	12.94	13.36	28.09	100

Fig. 4. Result of S/N ratio illustrating the influences
of factors on the displacement

S/N ratio values, the contribution of each factor was also achieved. Fig. 5 illustrates the contribution chart of the factors. As shown, the y coordinate of $\varnothing 100$ (factor F) was found to be the most important factor affecting displacement.
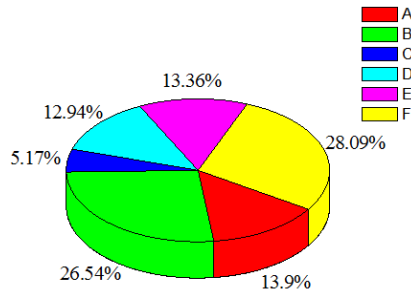

Fig. 5. Contribution of each factor from the S/N ratio results

In order to further study the contributions of the related factors, an ANOVA method was performed as described in Table 5. Similarly as in the S/N ratio analysis, the x coordinate of $\varnothing 28$ (factor B) and the y coordinate of $\varnothing 100$ (factor F) were found to be important factors concerning displacement reduction. There was a minor difference in the magnitudes of the factor contributions though there was a qualitatively alike trend apparent in the ANOVA and S/N ratio analyses. The ANOVA analyses showed only four factors, diameter $\varnothing 28$ (factor A), the x coordinate of $\varnothing 100$ (factor E), the x coordinate of $\varnothing 28$ (factor B) and the y coordinate of $\varnothing 100$ (factor F) as having bigger F values than $F_{(0.05,2,5)}$, consequently revealing that only these factors had statistically meaning.

Table 5.

Result of ANOVA

Parameters	S	f	V	F	$F_{(0.05,2,5)}$	P%	Rank
A	1.3357E-04	2	6.6785E-05	6.15036	5.78614	9.14	4
B	4.6493E-04	2	0.000232466	21.40824	5.78614	31.81	2
C	2.8001E-05	2	1.40004E-05	1.28932	5.78614	1.92	
D	1.1502E-04	2	5.75088E-05	5.2961	5.78614	7.87	
E	1.3948E-04	2	6.97397E-05	6.42247	5.78614	9.54	3
F	5.2626E-04	2	0.00026313	24.23217	5.78614	36.01	1
Error	5.4294E-04	5	1.0859E-05				
Total	0.00146	17					

4.1.3. Validation simulation

From the S/N ratio study, it was concluded that the minimum displacement could be achieved under the combination of A1-B3-C1-D3-E1-F3, as indicated in Fig. 4. Because of the geometry of the blade, this combination enlarges the shred-

ding head, and therefore minimizes the displacement. An additional simulation was performed using this combination as a validation test, revealing that the maximum displacement in the blade was 0.16209 μm. This value was smaller than the displacement results of all the cases listed in the orthogonal array in Table 3. Also, the boundary conditions of this simulation were the same as all 18 simulations listed in Table 3.

Figs. 6a and 6b present the displacement distributions under the combination set of Case 3 in Table 3 and the improved one from the S/N ratio study, respectively. From the validation simulation, it was confirmed that the Taguchi method resulted in better parameters for minimizing displacement.

(a) under the conditions of case 3

(b) under the new conditions from the S/N ratio analysis
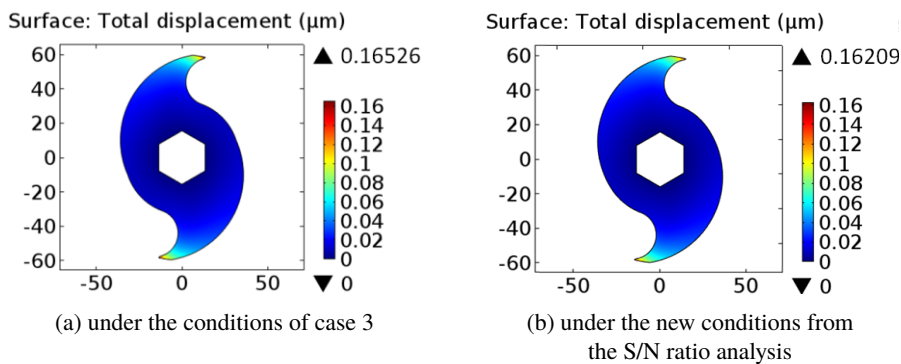
Fig. 6. Displacement distributions obtained by the numerical simulation

4.2. Optimization to minimize displacement

4.2.1. Developing response surface model

The Taguchi method is an effective and preeminent tool able to showing the relative significance of each factor and resulting in the improved set of the related dimensions for minimizing displacement [20]. However, the optimal values obtained from the Taguchi method were restricted to one of the three designated levels for each factor. Hence, RSM was used to further diminish the displacement of the shredding blade. In this investigation, the first-order response model was built utilizing the numerical results in Table 3. Utilizing the least-squares method, all the coefficients were derived, giving out the following simple model:

$$\text{Displacement} = 1.539 + 1.637 \cdot 10^{-2}\,A - 3.107 \cdot 10^{-2}\,B$$
$$+7.022 \cdot 10^{-3}\,C - 1.524 \cdot 10^{-2}\,D + 1.613 \cdot 10^{-2}\,E$$
$$+3.311 \cdot 10^{-2}\,F. \qquad (6)$$

From this model, factor F (the y coordinate of $\varnothing100$) was found to have the most important contribution because of its largest coefficient. Factor B (the

x coordinate of $\varnothing 28$) with the second largest coefficient had the second most important contribution. These values agreed with the previous S/N ratio analysis using the Taguchi method. It was worth noting that the first-order model also indicated factor A (the diameter $\varnothing 28$) to be more crucial than factor E (the x coordinate of $\varnothing 100$) concerning minimizing displacement. It can be attributed to the relatively small error (R^2 of 0.943) in the regression, showing that the current model can be optimized further, but not much.

$$\text{Displacement} = 252.314 - 1.567\,A + 4.623 \cdot 10^{-1}\,B$$
$$-2.282\,C - 4.721\,D + 1.354\,E - 6.269 \cdot 10^{-2}\,F$$
$$-2.769 \cdot 10^{-2}\,A^2 - 1.542 \cdot 10^{-2}\,B^2 + 2.601 \cdot 10^{-2}\,C^2$$
$$+2.353 \cdot 10^{-2}\,D^2 - 4.779 \cdot 10^{-2}\,E^2 + 1.479 \cdot 10^{-3}\,F^2\,. \tag{7}$$

It is worth noting that an R^2 value of 0.963 was defined for this model, thereby showing an improvement compared to the first-order model, but not much. It also showed a nonlinear regression with an acceptable error.

From this model, the response surface could be built for an imagination of the influences of the factors. Fig. 7 shows typical plots of the response surface of this investigation. The response surface with inspection for factor A (the diameter $\varnothing 28$) and C (the y coordinate of $\varnothing 28$) is illustrated in Fig. 7a. The response surface with inspection for factor D (the diameter $\varnothing 100$) and F (the y coordinate of $\varnothing 100$) is described in Fig. 7b. The lowest points, or minimum points, denote the optimal results for the corresponding factors.

A Q-Q plot using Matlab was employed, as illustrated in Fig. 8, to validate the current nonlinear regression and the obtained surface response model. This step

(a) A (the diameter $\varnothing 28$) and C
(the y coordinate of $\varnothing 28$)

(b) D (the diameter $\varnothing 100$) and F
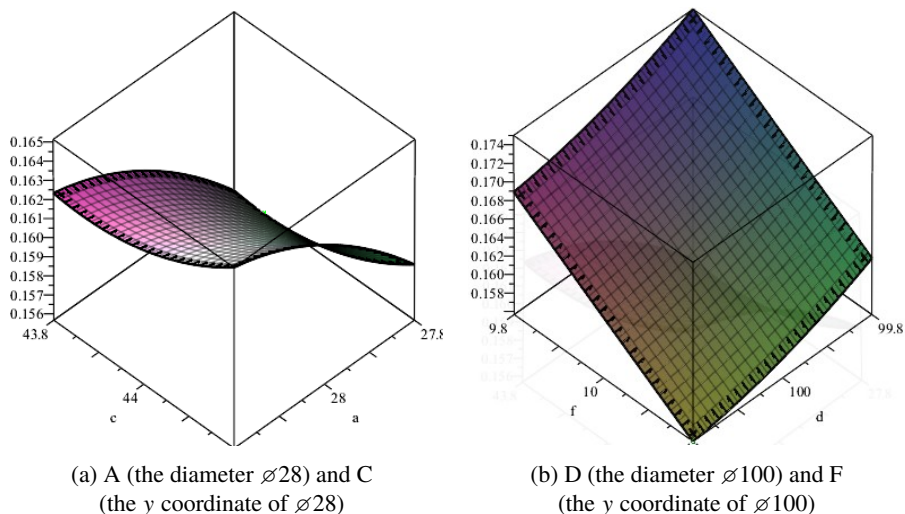(the y coordinate of $\varnothing 100$)

Fig. 7. Response surface of the displacement with respect to two factors

was not currently paid enough attention by other authors, which could have led to waste resources in inadequate RSM models. Fig. 8 proved that the generated model of this investigation was almost normally distributed.
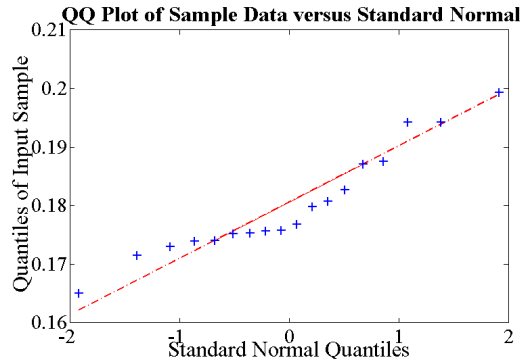

Fig. 8. Q-Q plot of the current response surface model

To define the optimum results of each factor and minimize displacement, the achieved surface response model was utilized. Fig. 9 describes the typical plots of S/N ratio and displacement obtained from the response model. As shown in Fig. 9b, both methods gave out the same optimum results for factor F (the *y* coordinate of $\varnothing 100$ mm). However, in the case of factor C (the *y* coordinate of $\varnothing 28$ mm), the RSM approach resulted in a more precise results than the S/N ratio analysis. In Fig. 9a, the two-segment line was the result of the Taguchi method while the curve was the result of the RSM. This clearly demonstrated the discrete nature of the Taguchi method. In other words, the result from the Taguchi method was bounded to one of the initial preset levels. As aforementioned, this advantage of the RSM approach over the S/N ratio analysis could provide a more finely tuned optimum results. Table 6 shows the optimum values for the factors of both approaches. A simple MATLAB$^{\circledR}$ script was then built and utilized to define the

(a) effect of factor C (the *y* coordinate of $\varnothing 28$ mm)

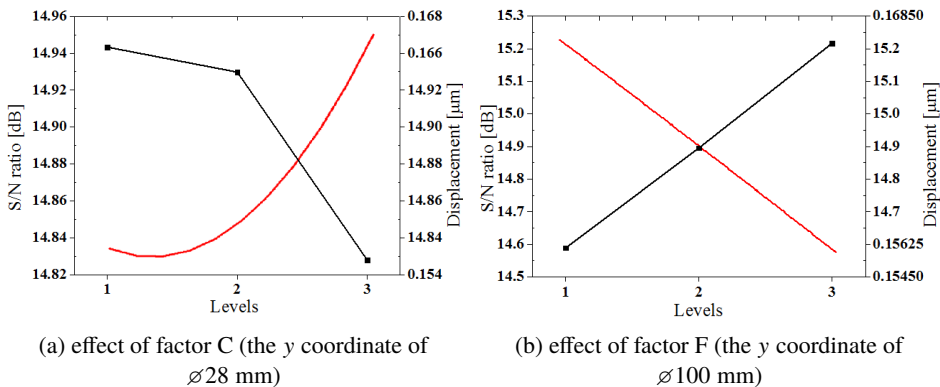(b) effect of factor F (the *y* coordinate of $\varnothing 100$ mm)

Fig. 9. Plot of both S/N ratio and warpage predicted from the second-order response model

optimum results from the second-order response model. The optimization function of Maple® has given out the same results as the MATLAB® script, consequently testifying the values. This proves that complicated algorithms as well as commercial software solutions can be forsaken by using a simple tool, such as MATLAB®, to carry out a study with minimal resources. It should be noted that the present script describes a simple approach to globalize the local optimization built-in module of MATLAB®.

4.2.2. Validation simulation using Comsol

To validate the optimal geometrical factors achieved using RSM, a confirmation simulation was performed (shown in Fig. 10). As shown in Table 6, the maximal displacement result of the shredding blades was determined to be around 0.162 μm, which was better (or smaller) than any other displacement values achieved in this investigation. This validation simulation showed that the current two-step optimization method efficiently provided improved optimum results by utilizing a minimal number of experiments, and without the need of using additional algorithms or software solutions.
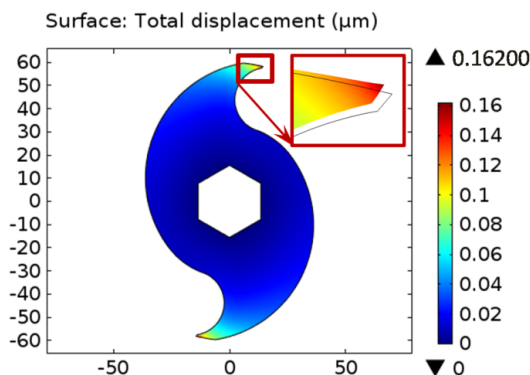

Fig. 10. Displacement distribution under the optimized geometrical factors

Table 6.

Recommended geometrical factors from the Taguchi method and RSM model

Symbol	Geometrical factors	Taguchi	RSM
A	Diameter ⌀28 (mm)	27.8	27.8
B	The x coordinate of ⌀28 (mm)	16.2	16.2
C	The y coordinate of ⌀28 (mm)	43.8	43.865
D	Diameter ⌀100 (mm)	100.2	100.2
E	The x coordinate of ⌀100 (mm)	13.8	13.8
F	The y coordinate of ⌀100 (mm)	10.2	10.2
Prediction values		N/A	0.15567
Validation results		0.16209	0.16200

It is worth noting that, when six factors are taken into account to build a second-order response model, Box-Behnken design and central composite design (CCD), which are commonly utilized DOE approaches, require 54 and up to 90 experiments, respectively. Therefore, the optimum combinations to obtain a minimum displacement of the shredding blade can be adequately achieved without any supplemental screening of geometrical factors.

4.2.3. Validation experiments

To validate the optimal geometrical factors obtained using the combination method, a validation experiment was carried out. In the experiment, two types of the shredding blades, the recommended combination from the Taguchi method and RSM, were used simultaneously. It was worth noting that the old shredding blades, which were previously used in the manufactory, were deformed easily, as shown in Fig. 11, after about five hours working continuously. Accordingly, the validation simulation results for these blades shown a rather large deformation, 0.28625 μm.
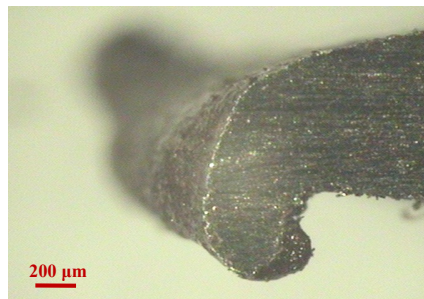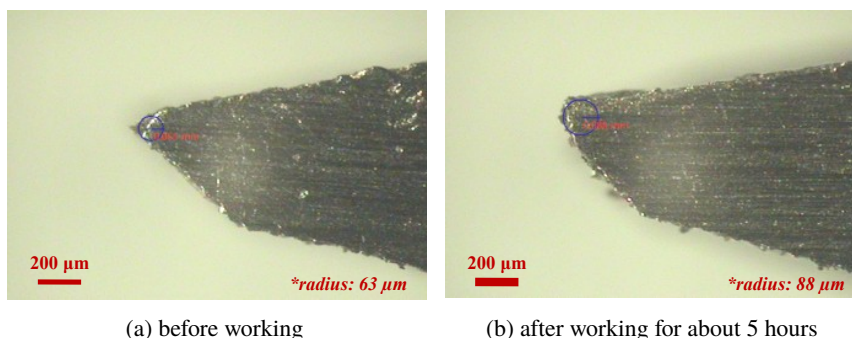

Fig. 11. Photograph of the previously used shredding blade
via Icamscope®

The two new types of the blade were then also measured via microscope after about five hours working continuously. Figs. 12a and 13a show the dimensions of the shredding head of the blade from the Taguchi method and RSM, respectively,

(a) before working   (b) after working for about 5 hours

Fig. 12. Photograph of the shredding blade from Taguchi method via Icamscope®

before working. The dimensions of them were almost the same (63 μm compared to 62 μm). Figs. 12b and 13b show the dimensions of them after about five hours working continuously. The radius of the shredding head of the blade from the Taguchi method increased to 88 μm while the one from RSM was 71 μm. This result verified an improvement experimentally.
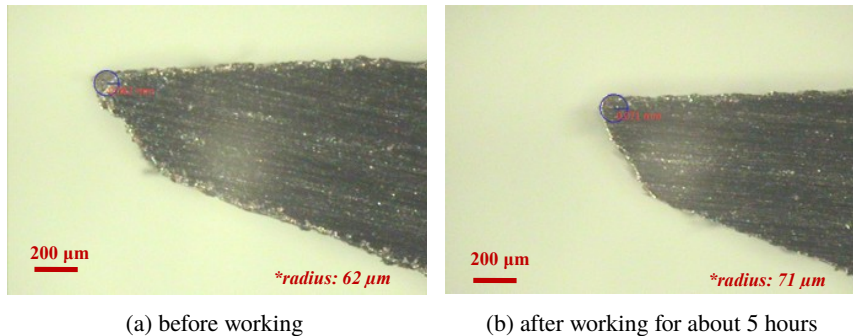

(a) before working	(b) after working for about 5 hours

Fig. 13. Photograph of the shredding blade from RSM via Icamscope®

Hence, it was verified, both numerically and experimentally, that the simple integration of the Taguchi method and RSM was effective enough to overcome the drawbacks of the Taguchi method as a discrete optimization one and to calculate better values in regimes without utilizing other complicated algorithms or software solutions.

5. Conclusions

In the current investigation, a two-step optimization approach was utilized to study the influences of geometrical parameters on the displacement of the shredding blade of a plastic waste shredder, and also to define the optimum combination for minimum displacement. The optimization approach employed in this investigation consisted of the orthogonal array and ANOVA of the Taguchi method used in combination with RSM. In the numerical simulations of the blade with shredding load, six geometrical factors were considered. Using the S/N ratio analysis and ANOVA based on the Taguchi method with an $L_{18}(3^6)$ orthogonal array, the y coordinate of $\varnothing 100$ mm and the x coordinate of $\varnothing 28$ mm were found to be the most important factors for minimization of displacement of the shredding blade. RSM was put on the values of the Taguchi analysis with a second-order nonlinear regression model to determine the ideal values of the geometrical factors. A short script was also developed to globalize the local optimization built-in module of MATLAB® to numerically obtain the optimum results from the RSM. Using the blade design by RSM, the numerically validation results showed an improvement of 43.41%, 1.97%, and 0.06% compared to the original blade, the best in the set of 18 combinations in Table 3, and the blade designed by the Taguchi method, respectively.

A new set of blades with optimized geometry was then fabricated and experimented, showing lower wear via measurement by an ICamScope®microscope. By this, the optimum factor values were adequately achieved and testified via both the numerical simulations and the on-site experiments.

The simple but excellent presentation of the two-step optimization utilized in this investigation can prove its benefit in many manufacturing technologies of medium and small scale manufactories, where commercial optimization software solutions are not always available. Moreover, the usefulness of the current method is also hoped to fill the gap between academic investigation and industrial manufacturing.

Acknowledgements

References

[1] S. Alavi, S. Thomas, K.P. Sandeep, N. Kalarikkal, J. Varghese, and S.Yaragalla. *Polymers for Packaging Applications*. Apple Academic Press, 2014.

[2] A.W. Ayo, O.J. Olukunle, and D.J. Adelabu. Development of a waste plastic shredding machine. *International Journal of Waste Resources*, 7(2):1-4, 2017.

[3] P.K. Farayibi. Finite element analysis of plastic recycling machine designed for production of thin filament coil. *Nigerian Journal of Technology*, 36(2):411–420, 2017. doi: 10.4314/njt.v36i2.13.

[4] S. Reddy and T. Raju. Design and development of mini plastic shredder machine. *IOP Conference Series: Materials Science and Engineering*, 455:012119, 2018. doi: 10.1088/1757-899x/455/1/012119.

[5] D. Atadious and O.J. Oyejide. Design and construction of a plastic shredder machine for recycling and management of plastic wastes. *International Journal of Scientific & Engineering Research*, 9(5):1379–1385, 2018.

[6] Y.M. Sonkhaskar, A. Sahu, A. Choubey, A. Singh, and R. Singhal. Design and development of a plastic bottle crusher. *International Journal of Engineering Research & Technology*, 3(10), 297–300, 2014.

[7] M.I. Faiyyaj, M.R. Pradip, B.J. Dhanaji, D.P. Chandrashekhar, and J.S. Shivaji. Design and development of plastic shredding machine. *International Journal of Engineering Technology Science and Research*, 4(10):733–737, 2017.

[8] S.B. Satish, J.S. Sandeep, B. Sreehari, and Y.M. Sonkhaskar. Designing of a portable bottle crushing machine. *International Journal for Scientific Research & Development*, 4(7):891–893, 2016.

[9] N.D. Jadhav, A. Patil, H. Lokhande, and D. Turambe. Development of plastic bottle shredding machine. *International Journal of Waste Resources*, 08(2):1000336, 2018. doi: 10.4172/2252-5211.1000336.

[10] T.A. Olukunle. Design consideration of a plastic shredder in recycling processes. *International Journal of Industrial and Manufacturing Engineering*, 10(11):1838–1841, 2016. doi: 10.5281/zenodo.1127242.

[11] A. Tegegne, A. Tsegaye, E. Ambaye, and R. Mebrhatu. Development of dual shaft multi blade waste plastic shredder for recycling purpose. *International Journal of Research and Scientific Innovation*, 6(1):49–55, 2019.

[12] J.M.A. Jaff, D.A. Abdulrahman, Z.O. Ali, K.O. Ali, and M.H. Hassan. Design and fabrication recycling of plastic system. *International Journal of Scientific & Engineering Research*, 7(5):1471–1486, 2016.

[13] S. Yadav, S. Thite, N. Mandhare, A. Pachupate, and A. Manedeshmukh. Design and development of plastic shredding machine. *Journal of Applied Science and Computations*, 6(4):21–25, 2019.

[14] S. Ravi. Utilization of upgraded shredder blade and recycling the waste plastic and rubber tyre. *International Conference on Industrial Engineering and Operations Management*, pages 3208–3216, Paris, France, 26-27 July 2018.

[15] M.F. Nasr and K.A. Yehia. Stress analysis of a shredder blade for cutting waste plastics. *Journal of International Society for Science and Engineering*, 1(1):9–12, 2019. doi: 10.21608/jisse.2019.20292.1017.

[16] C. Pedraza-Yepes, M.A. Pelegrina-Romero, and G.J. Pertuz-Martinez. Analysis by means of the finite element method of the blades of a PET shredder machine with variation of material and geometry. *Contemporary Engineering Sciences*, 11(83):4113–4120, 2018. doi: 10.12988/ces.2018.88370.

[17] A. Ikpe and O. Ikechukwu. Design of used PET bottles crushing machine for small scale industrial applications. *International Journal of Engineering Technologies*, 3(3):157–168, 2017. doi: 10.19072/ijet.327166.

[18] N.Y. Mahmood. Prediction of the optimum tensile – shear strength through the experimental results of similar and dissimilar spot welding joint. *Archive of Mechanical Engineering*, 67(2):197–210, 2020. doi: 10.24425/ame.2020.131690.

[19] R. Świercz, D. Oniszczuk-Świercz, and L. Dąbrowski. Electrical discharge machining of difficult to cut materials. *Archive of Mechanical Engineering*, 65(4):461–476, 2018. doi: 10.24425/ame.2018.125437.

[20] T.K. Nguyen, C.J. Hwang, and B.-K. Lee. Numerical investigation of warpage in insert injection-molded lightweight hybrid products. *International Journal of Precision Engineering and Manufacturing*, 18(2):187–195, 2017. doi: 10.1007/s12541-017-0024-5.

[21] T.K. Nguyen and B.-K. Lee. Investigation of processing parameters in micro-thermoforming of micro-structured polystyrene film. *Journal of Mechanical Science and Technology*, 33(12):5669–5675, 2019. doi: 10.1007/s12206-019-1109-0.

[22] T.K. Nguyen, A.-D. Pham, M.Q. Chau, X.C. Nguyen, H.A.D. Pham, M.H. Pham, T.P. Nguyen, and H.S. Nguyen. Development and characterization of a thermoforming apparatus using axiomatic design theory and Taguchi method. *Journal of Mechanical Engineering Research and Developments*, 43(6):255–268, 2020.

[23] R.O. Ebewele. *Polymer Science and Technology*. 1st edition. CRC Press, Boca Raton, 2000. doi: 10.1201/9781420057805.